THE EFFECT OF EXTERNAL BLAST ON CYLINDRICAL STRUCTURES

D.M. Brown* and P.F. Nolan*

The resistance of common chemical plant items to blast loadings was studied by subjecting scale models of cylindrical plant items to simulated vapour cloud explosions. The resulting blast loadings deformed the instrumented models both elastically and plastically. The theories developed for similar circumstances of dynamically applied loads were used to evaluate the experimental results. The effects of the magnitude of the peak pressure and the total impulse of the wave were examined as well as height to diameter ratio of the models, position of models in relation to the oncoming blast loading and the additions of stiffening rings and wind spoilers.

INTRODUCTION

It has been suggested that when a vapour cloud is mixed with air in the open and is ignited a number of situations may arise, these include

(i) a burning action where the cloud simply burns at relatively low burning velocities (< 2.0 m sec^{-1}) generating no significant pressure disturbance but a "fireball". This is a characteristic mushroom shape of burning vapour which can generate considerable heat.
(ii) a deflagration where the cloud's initial laminar or steady burning velocity is accelerated and a pressure wave is generated ahead of the flame which can be either subsonic or supersonic in velocity.
(iii) a detonation where a strong blast wave is produced as the reaction front propagates through the reactants.

There has been some debate as to whether a true detonation has ever occurred in an industrial explosion (1,2,3). In a deflagration the flame front propagates through the combustible material at a speed related to the normal "burning velocity" of the mixture. The burning velocity can be enhanced by

(a) expansion of the volume of the reaction products

(b) turbulence caused by air entrainment at the release point and the presence of obstacles.

In most of the industrial incidents the term "unconfined vapour cloud explosion" has been misleading since a degree of confinement has existed, due to the presence of process plant. Their presence may enhance the magnitude of associated pressure

*Department of Chemical Engineering, Polytechnic of the South Bank, Borough Road, London SE1 OAA.

effects by reflections and/or the acceleration of flame. A vapour cloud explosion produces a smaller over-pressure than that produced by a conventional condensed explosive. It is, however, of longer duration and may produce more damage.

A number of design codes (4,5,6) exist for plant items. Such codes consider the effects of the weight of the vessel, operating pressures and prevailing wind loadings. A procedure for blast loading design is not usually included. Guidance does exist on the blast resistant design of control rooms (7,8). A simple model for the response of structures to blast loadings exists (9). The method assumes that a structure can be represented as a one degree of freedom system and applies mainly to rectangular, shaped buildings. The conditions relating to tall, slender chemical plant items are fundamentally different to those of rectangular structures. The initial "diffraction" (i.e. the difference in pressure loadings on the front and back of a structure) loading of the shock is quickly equalised around the back of the structure. Cylindrical columns are susceptible to the "drag" phase of the loading from the ensuing blast wind. This is much longer in duration and therefore potentially more destructive.

Techniques for describing and calculating elastic and plastic deformations for thin cantilevers subjected to blast waves from condensed explosives are available in the literature (10). The duration of the loading compared with the natural frequencies of the cantilevers is short and the analysis is derived for an impulsive type loading. Following the incident at Flixborough, Roberts (11) developed a simple model to explain the damage caused to the lamp-posts on the site. This model takes into account the impulse and duration of the loading. The analyses of other industrial incidents have used the equations for static collapse loading. Jones (12) adapted a mode summation technique based on a quasi-static loading assumption to explain the experimental work of Pritchard (13) which concerned the calculation of damage caused to cantilevers under time varying loading patterns resulting from a flammable gas/air explosion.

EXPERIMENTAL PROGRAMME

The aim of the work was to investigate plant damage due to external blasts. An explosion gallery at the Health and Safety Executive's Explosion and Flame Laboratory at Buxton was used which consisted of a cylindrical, hollow steel tunnel, 69m in length and 1.2 m in diameter. The gallery was closed at one end where a polythene envelope was suspended from the inside of the walls. A flammable mixture of methane and air was fed into the envelope. This mixture was approximately in stoichiometric proportions and was between 4 and 9 m^3 in volume. It was ignited using powdered fuses and the resulting pressure disturbance in the form of a weak shock wave travelled towards the open-end of the gallery. The gallery was constructed from eight cylindrical sections and in each section pressure transducers (Bell and Howell type 4-326-1471) and photo-electric cells enabled measurement of pressure variations and the arrival of the flame/shock front. The shock reached a maximum peak value in the third section from the closed end. The peak value then decayed as it travelled towards the open end. The duration of the positive phase of the pulse increased up to a steady value from sections 1 through to 5 and then remained at a constant value (0.125 sec). The speed of the shock front had an average value of 470m sec^{-1} derived from the photocell and pressure transducer readings.

In the fifth section from the closed end of the gallery the scale models or replicas of the vertical cylindrical chemical plant items were attached to a steel bench traversing the bottom of the gallery. The models were approximately 1/40th of the industrial scale. All had a diameter of 19 mm and wall thickness of 0.254 mm with heights varying between 370 and 900mm. They were fabricated from stainless steel (ASTM-A-269-75, AISI 316). The tops of all the columns were tori-spherical and held in position by a base "plug" system. A mild steel plug 95mm in length was inserted

inside the replica and provided a tight fit. The shaped bottom of the plug fitted into one of a series of holes drilled into the bench. These holes were spread over the bench to enable the effect of position of a single model to be determined as well as to allow the use of a number of models simultaneously in a range of configurations.

The models were instrumented with strain gauges (WSG CEA-06-062UW-350 and CEA-06-062UR-350) to enable measurements and subsequent calculations of elastic deformation, applied strain rate and principal stresses. A small number of the models were fitted with scaled versions of stiffening rings and wind spoilers.

In order to measure the actual loadings on the models a rigid replica was made with the same external dimensions. This accommodated three miniature pressure transducers (Kulite CQ-140-100A). These small transducers were housed in demountable brass sections held in position by a silicon rubber compound. The brass sections could be situated at various positions in the rigid steel replica by using different interconnecting lengths.

The associated wiring passed down the hollow centre section of the brass inserts. This rigid replica meant that the transducers could be positioned at varying heights in the gallery and could be rotated to face any direction i.e. the variation of pressure with height in the gallery could be studied. In the range of heights utilised in the tests, the peak over-pressure on the rigid replica remained constant.

It was expected that the fifth section of the gallery was sufficiently removed from the open-end of the gallery to minimise complications caused by reflection of the pressure disturbance. (i.e. end effects) This fifth section contained sight glasses to enable the use of a 16 mm cine camera to film the deflections of the models. Also in section 5, a rigidly mounted gauge was used to measure the stagnation pressure in the centre of the section and a piezo-electric pressure gauge (Kiag 7507 SN 98935) mounted in the top of the gallery allowed the measurement of the side-on over-pressure. The applied dynamic load was measured by using a reed anemometer. The reed was a thin steel beam with a strain gauge (WSG CEA-06-062UW-350) attached. The beam was elastically deformed by the blast wind of the explosion.

It was necessary for the application of the analytical techniques to determine the yield stress and associated moment for the material. Stainless steel does not exhibit a definite yield point and a 0.2% proof stress was obtained using a "Mayes" tester. The 0.2% proof stress was found to be 566.8 MPa, which is equivalent to a moment of 35.87 Nm^{-1}. The Young's Modulus was estimated at 205.9 10^9 Pa.

The actual elastic deformations of the replicas were obtained from the high speed cine records or strain gauge readings and applying the equation:

$$\epsilon = E/kVN$$

where ϵ = strain

E = gain from amplifier

k = gauge factor

N = number of active bridge arms.

The deflection from the vertical was calculated from

$$\tan \theta = x/L$$

where L = height of cylinder

x = distance the tip is deflected from the original position

Stainless steel is strain rate sensitive and becomes apparently stronger with increase in the applied strain rate. The method developed by Cowper and Symonds (14) was used to calculate the strain rate.

An assumption of the experimental programme was that the pressure vs. time signature resulting from an industrial incident was represented by the pressure pulse generated in the gallery. Currently, no measured data is available relating pressure histories from full-scale unconfined vapour cloud explosions. The magnitude of shock waves needed to cause the observed damage in previous incidents has been estimated as overpressures of up to several bar (15,16). At Flixborough, Sadee et al (17) estimated overpressures of up to 1 bar and Clancey (18) suggested localised pressures resulting from confinement in the region of 5 to 7 bar. In the experimental programme, the positive phase durations were in the range of 0.09 to 0.19 seconds and rise times varied between 0.01 and 0.085 seconds. Pressures up to 1.5 bar were observed in the gallery.

EXPERIMENTAL RESULTS

Measurements were made of

(a) peak dynamic pressure recorded by reed anemometer, P_R (kPa).

(b) peak stagnation pressure registered by stagnation gauge, P_S (kPa).

(c) peak side-on over-pressure in section 5 measured by piezo-electric gauge, P_{5A} (kPa)

(d) peak side-on over-pressure in Section 5 measured by transducer in side-wall, P_{5B} (kPa)

(e) peak side-on over-pressure in section 1, P_1 (kPa)

(f) peak pressure experienced by the miniature pressure transducers situated in the wall of the rigid replica directly facing the oncoming shock wave P_{F1} and P_{F2} (kPa)

(g) peak pressure loading (miniature pressure transducers) on the reverse side of the rigid relica, P_{B1}, P_{B2}, P_{B3} (kPa)

(h) rise time in seconds of the pressure pulse, t_1 (sec.)

(i) duration of the positive phase of the pulse, t_2 (sec.)

(j) maximum output of the strain gauges affixed to the replicas S (volts)

Table 1 lists some examples of the experimental results from the total of 260 ignitions. The majority of experiments involved the use of one replica. In the cases employing more than one model, various configurations of the positioning on the bench were used.

It can be seen that a uniform loading pattern occurred throughout the height of the column except immediately above the bench surface. This was due to the shock interaction with the leading edge of the cross-member.

Table 1

Typical experimental results

RUN	P_R	P_S	P_1	P_{5A}	P_{5B}
	kPa	kPa	kPa	kPa	kPa
123	16.08	84.38	63.53	69.48	68.37
124	17.47	77.14	58.78	61.36	61.52
127	23.64	112.41		89.25	83.29
135	9.66	59.18	48.62	49.34	48.46
136	34.51	163.22	118.61	129.03	125.63
145	24.84	117.32	76.01	84.18	82.34
158	11.38	68.22	51.86	56.34	56.74
182	10.48	51.68	34.29	39.36	37.64
185	12.71	57.26	41.57	43.10	43.63
189	13.42	68.62	52.15	55.34	54.81
210	23.82	101.62	75.34	81.93	80.45
212	11.94	45.94	33.52	33.67	38.27
214	14.5	65.21	51.47	52.78	55.16
225	19.68	64.45	51.64	49.37	51.66
231	23.48	82.87	56.34	53.47	57.26
238	16.48	69.06		55.82	56.33
240	14.19	66.76		55.81	56.24
242	10.03	48.31		39.43	40.21
243	23.07	55.25		44.14	43.28
245	20.75	75.89		62.31	63.70

RUN	P_{F1}	P_{F2}	P_{B1}	P_{B2}	P_{B3}	t_1	t_2	S
	kPa	kPa	kPa	kPa	kPa	sec	sec	volts
123	93.13		56.92			0.042	0.125	
124	75.26		75.26			0.031	0.068	5.24
127	111.91		85.81			0.023	0.162	
135	60.33		46.23			0.047	0.158	0.41
136	167.6		117.35			0.047	0.109	4.82
145	122.29		81.42			0.035	0.177	
158	67.36		52.61			0.090	0.291	0.51
182	53.25	52.98	35.23			0.025	0.17	
185	58.65	57.84	36.21			0.033	0.172	
189	69.34	75.92	43.43			0.032	0.169	
210	101.43	97.98				0.015	0.097	12.5
212	46.5	46.2	33.91			0.034	0.169	
214	58.31	64.23				0.032	0.142	
225				38.23	37.58	0.063	0.220	
231				51.06	48.24	0.051	0.205	
238				41.26	38.64	0.032	0.172	1.2
240				41.01	42.1	0.04	0.196	0.09
242				33.17	34.01	0.05	0.151	2.30
243				28.76	28.94	0.068	0.204	3.47
245				47.03	48.22	0.023	0.164	0.61

Table 2 lists some typical values for the damage caused to the replicas expressed as both a tip deflection γ and the deflection from the original vertical position, Θ degrees. For those models, which did not deform plastically an estimate of the strain is given.

Table 2

Typical damage to models.

Run	Length m	Angle degrees	Tip displacement m	Strain
117	0.37	1.0	0.006	8.11×10^{-4}
118	0.585	104	0.59	3.34×10^{-3}
124	0.6	2	0.021	2.91×10^{-3}
182	0.705	95.1	0.705	
185	0.505	22	0.005	
200	0.505	1.2	0.011	
205	0.505	0	0	1.2×10^{-3}
210	0.655	94	0.655	3.12×10^{-3}
214	0.415	0	0	0.9×10^{-3}
217	0.585	107	0.585	3.15×10^{-2}
219	0.605	1.4	0.015	
225	0.505	69	0.475	
226	0.605	1.1	0.011	4.6×10^{-3}
228	0.705	64	0.636	
231	0.705	102.5	0.705	
232	0.505	1	0.008	
238	0.705	75	0.684	
241	0.705	78	0.705	

ANALYTICAL TECHNIQUES

The analysis of the damage sustained by the models in this study consisted of

(i) application of the Roberts' approach
(ii) application of a modified mode summation technique
(iii) utilisation of a P-I diagram

(i) The Roberts approach

This approach allows the impulse necessary to reach the static collapse moment of a structure to be calculated. It assumes that the drag phase of a blast loading causes the damage to slender shapes. The approach requires a number of assumptions to be made, these include.

(a) an idealised stress/strain relationship and that the material is "perfectly plastic"
(b) the applied loading exerted on the structures does not vary with time but is finite in duration.

(c) the applied loading is constant along the length of the structure

The Roberts approach was used to calculate the uniform load per unit length. These calculations involved the use of a strain rate corrected value for the yield moment (M_o) and values of the applied moment (M) for the angle of deformation derived from a static bending test and then corrected for strain rate. Typical results are given in Table 3. The length of the model was 0.605m and the duration of the positive phase was 0.08 sec.

Table 3

Typical values of the applied load

Run	Applied Load $N\ m^{-1}$ M_o=35.8 Nm^{-1}	Applied Load $N\ m^{-1}$ M vs θ
97	403.86	403.86
111	729.85	729.85
113	733.46	733.46
114	249.71	345.64
116	624.15	833.91
117	287.57	287.57
118	336.23	427.26
124	283.71	283.71
127	224.69	323.54

(ii) The mode summation technique

Jones (12) utilised existing techniques to calculate the damage to cantilevers subjected to a dynamic loading. The technique requires the determination of the frequencies, application of the modified Rayleigh method and Lagranges equation. It is possible to calculate the elastic deformation, the strain rate corrected yield moment and tip deflection. The technique assumes that the material is perfectly elastic up to its yield point and then behaves in a rigid plastic manner. No allowances are made for strain hardening and the "true" stress/strain relationship of the material. The plastic phase model utilises the proposals made by Symonds (19).

Examples of the elastic and permanent tip deflections using the mode summation technique are presented in Table 4. The letters R and T indicate the use of experimental data from the reed anemometer and miniature pressure transducers.

Using the mode summation technique for experimental run 97 with the model of height 0.505m, the peak load is 450 Nm^{-1}, the time (t_1) to reach the peak is 0.024 sec and the positive phase duration (t_2) is 0.093 sec. It is possible to calculate the time to attain the strain rate corrected value for the yield moment by iteration and this is found to be 0.0216 sec with the corresponding value of the applied load as 432 N m^{-1}. The mode velocity $d\gamma/dt$ of the tip at this stage is 2.16 m sec^{-1} and the time elapsed for the model to come to rest is 0.0254 sec. The final tip displacement is 0.064m.

Table 4

Typical values of the tip deflection calculated by the mode summation technique

Run	Tip deflection based on dynamic pressure m (R)	Tip deflection based on dynamic pressure m (T)	Elastic tip deflection m (R)	Elastic tip deflection m (T)
135	0.00	0.88	0.0062	0.0163
159	0.59	1.34	0.0095	0.0146
200	1.62	3.27	0.0123	0.0151
205	0.00	0.00	0.0124	0.0162
213	0.34	0.58	0.0100	0.127
219	0.00	1.77	0.0105	0.0138

(iii) P-I diagram (20)

The peak load/impulse characterisation diagram is used to compare experimental and theoretical results of "pulse" loaded systems. Combinations of peak load, P and impulse, I which cause the same degree of damage to a structure are plotted as an iso-damage curve. Figure 1 illustrates a P-I diagram for the case of varying extents of permanent deflections on replicas of height 0.605 m, based on theoretical predictions using the Roberts approach. On the same diagram, the actual experimental loadings experienced by models of the same height are shown.

DISCUSSION

The peak loadings experienced by the models were between 150 N m^{-1} and 780 N m^{-1}, with applied strain rates reaching up to 1.6 strain $sec.^{-1}$. The observed damage to the models could be divided into three main types:-

(i) models, which were "deformed" elastically only, and which exhibited no signs of permanent deformation

(ii) models, where the yield point was exceeded, which underwent a relatively small plastic deformation, with the test structures bending through an angle of up to 5 degrees only.

(iii) models, where the extent of plastic damage was large, resulting in buckling of the specimens and bending in excess of 85 degrees from the vertical.

ELASTIC DEFORMATIONS

Elastic deformation occurred when

(i) the peak over-pressure values were relatively low

or

(ii) the models were less than 0.45 m in height.

The relevant principal stresses and elastic deformations were calculated from the voltage outputs of the strain gauges.

SMALL PLASTIC DEFORMATIONS

Some models were "deflected" through angles varying from 1 to 3 degrees, with corresponding tip deflections of between 3 and 19 mm. The models deformed in this way varied in height between 0.465 and 0.8 m. No definite buckling point was indicated on the deformed structure i.e. no significant change in cross-section of the models was apparent. Table 5 lists the loadings required to deform replicas of varying heights through small deflections. The loadings are expressed in terms of the dynamic pressure, q_s recorded by the reed anemometer.

Table 5

Typical peak loadings which caused small angle deflections

RUN	LENGTH m	ANGLE ^{o}	Loading N m^{-1}
117	0.59	1.0	210
135	0.73	1.5	184
185	0.505	2.0	242
188	0.505	3.0	260
214	0.515	1.1	276
227	0.505	1.2	256
233	0.405	1.0	288
234	0.605	1.5	226

LARGE PLASTIC DEFLECTIONS

Approximately 50% of the models were buckled and their final deformed shapes were bent from 85 to 116 degrees away from the original vertical position. The corresponding tip deflections varied from 0.385 to 0.795 m. The cross-sections of the models were altered dramatically in the region where the buckling process occurred, changing from originally circular geometry to almost flat profiles. A complex series of "folds", built-up as the structure collapsed upon itself. These occurred at the back of the test specimens (i.e. that part not directly facing the blast), caused by the compression forces initiated by the buckling action. On the opposite face, the tensile or stretching forces of the applied loading caused a "diamond" shaped deformation.

INTERMEDIATE PLASTIC DEFLECTIONS

A comparatively small number of test structures were deflected between 5 and 85 degrees. Table 6 lists the range of peak dynamic loading.

SPECIAL CASES

In two specimens, rupture of the skin of the models was evident. In the vicinity of the buckling area of the models very fine cracks appeared. The loadings recorded from the miniature pressure transducers were 630.9 N m^{-1} and 640.1 N m^{-1}. These loadings are high but not exceptional, since loadings of 780 N m^{-1} were obtained. The stress pattern illustrated that the specimens had been subjected to a relatively high strain rate.

Table 6

Peak loadings which caused intermediate deflections.

RUN	LENGTH m	ANGLE degrees	LOADING $N\ m^{-1}$
71	0.42	22	295
159	0.65	74	234
228	0.80	64	335
238	0.80	75	313
240	0.805	71	270
241	0.80	78	202

INFLUENCE OF REPLICA CONFIGURATION

The positions of the models on the steel cross-member (bench) traversing the inside of the gallery were varied. The extent of deformation of models was not influenced by their relative positions in the various configurations. It might have been expected that a degree of protection would be afforded by the leading model when positioned in front of another. This was not however, the case.

ADDITION OF SPOILERS

Tall, slender columns in industrial plant are often fabricated with the addition of a spoiler attached to their outer surface. Its purpose is to dissipate the effect of wind loadings on the column. The spoilers are designed to operate effectively at the *Reynolds' numbers derived from the range of prevailing wind speeds and their fre*quency in a particular location. In general, under dynamic pressure loadings observed in the tests, it was found that for a given height, a smaller loading is required to deform columns with wind spoilers attached to them. This effect is mainly a consequence of the increased projected area caused by the addition of the spoilers which increase the effective loading on the structure under the experimental conditions.

ADDITION OF STIFFENING RINGS

It is often necessary to include "stiffening rings" in the design and subsequent fabri*cation of columns. These can enhance the strength of a given column and signifi*cantly modify the fundamental modes of vibration of a structure. Comparison of models with and without stiffening rings showed that as would be expected, applied loadings needed to be substantially increased to cause similar damage to models with stiffening rings.

HEIGHT TO DIAMETER RATIO

Figure 2 indicates that an increase in L/D ratio for the models increased the likli*hood and degree of deformation for a given loading.*

THE ROBERTS' APPROACH

Figures 3 and 4 illustrate plots of actual loadings versus those predicted using the approach presented by Roberts and Pritchard (11). Figure 3 is a plot of calculated load versus dynamic pressure readings, while Figure 4 utilises values from the minia-

ture pressure transducers. Only a small proportion of the results gave a large deviation from the predicted loadings estimated by the following equation

$$\hat{\theta} = \left[\frac{3q}{4m_1}\right] t_d^2 \left[\frac{qL^2}{2m_o} - 1\right]$$

where

$\hat{\theta}$ = permanent angular displacement
q = uniform load per unit length
m_1 = mass per unit length
L = height
t_d = duration of positive phase of loading
M_o = yield moment

also

$$\frac{\theta}{\theta_d} = \frac{qL^2}{2M_o}$$

where $\theta_d = \theta$ at $t = t_d$

The intrinsic random variation in experiments on blast damage is large and the scatter on Fig. 3 correspondingly great. The statistical analysis conducted takes account of the fact that we have no prior knowledge of the magnitude of the actual dynamic load and the calculations are made without recourse to adjustable parameters that can be fitted to correlate the data. The first analysis was to establish whether the calculations gave answers of the right order of magnitude. For this purpose we compared the hypothesis: Actual Dynamic Load = 0, with the hypothesis Actual Dynamic Load = Calculated Dynamic Load.

The deviation of the measurement from zero is measured by s(y), where s(y) is $(y_1^2 + y_2^2 .. y_n^2)/n$; n observations. The deviation from the prediction is similarly measured by s(y-x), i.e. $[(y_1-x_1)^2 + (y_2-x_2)^2 + \ldots]/n$. The values obtained are s(y) = 89600 and s(y-x) = 55800. s(y-x) is significantly less than s(y) which shows that the calculated load is a good order-of-magnitude predictor of the measured dynamic load. We next test whether there is correlation between the calculated and measured values. If the relationship between x and y is purely random, then it would be expected that $s(y-x) = \hat{s}(y-x) = s(y) + s(x) - 2\bar{x}\bar{y}$; for positive correlation s(y-x) is less than $\hat{s}(y-x)$. The values obtained are $\hat{s}(y-x) = 62200$. s(y-x) is less than $\hat{s}$ which shows that there is a significant correlation. In view of the wide scatter of the experimental results, more sophisticated statistical analysis not justified, it is sufficient to conclude that Roberts' relationship gives order-of-magnitude prediction of actual dynamic loads.

The correlation for the miniature pressure transducers (Fig.4) is much stronger. Corresponding values are s(y-x) = 12300, s(y) = 208900, $\hat{s}(y-x)$ = 39700. Using the calculated loadings to predict the M.P.T. readings reduces the variance by over 94% compared to the null prediction. The correlation is also high, the variance of (y-x) being only 30% of that expected if the relationship had been random. These M.P.T. results were sufficiently well correlated to make further analysis worthwhile. For this analysis the data were logarithmically transformed (having the affect of weighting the observations as $1/y_i^2$, which we believe reflects the experimental precision). In this case we find that the best straight line through the origin is, within 1%, y=x, which confirms the value of the prediction.

MODE SUMMATION METHOD

Figure 5 illustrates a plot of predicted elastic deflections versus those estimated from the output ofthe strain gauges attached to the replicas. A statistical analysis similar to that conducted for Fig. 4 was undertaken. Again good order of magnitude prediction was obtained. The value of $s(y-x)$ is less than $s(y-\tilde{y})$ which demonstrates a significant correlation [note, in fitting the mean y a degree of statistical freedom is used so that, for a random set of results it would be expected that $s(y-\tilde{y})$ would be considerably less than $s(y-x)$]. Regression showed that the best straight line through the origin is $y = 1.18x$. The standard deviation about the line $y=x$ is less than 5% greater than about the "best" line. We conclude that, within the intrinsic reproducibility of the measurements, the deflections calculated by the mode summation method are in agreement with the experimentally mesured tip displacement.

The comparison between theory and experimental observations for small plastic displacements is shown in Figure 6.

The cause of the discrepancies for large angle deflections was the physical constraints on the models which prevented them from "deforming" through greater tip deflections than those observed. The analysis does not take into account the complex buckling process, which introduces membrane forces in the vicinity of the collapse of the cross-section of the cylinder. The method also relies on an idealised triangular shape pressure loading pulse on the structure. In particur the analysis proved very sensitive to the rise time. In the actual analysis the time taken to reach the yield point was less than the rise time, varying from 0.0097 to 0.03 sec. The corresponding mode velocities of the tips of the cylinders were in the range 0.12 to 11.6 m sec^{-1}. Final tip deflections varied from 0.314×10^{-3} to 12.6 m.

P-I DIAGRAM

Figure 1 illustrated the P-I diagram for the models. The curves shown are for small angle (1°) and large angle (90°) deflections for models of length 0.605 m. and a typical positive phase duration of 0.01 sec. The diagram also illustrates some of the difficulties encountered in this type of experimental programme. Referring to the asymptote adjacent to the horizontal "Impulse" axis, it is evident that for plastic deformations a relatively small change in applied peak loading can give a correspondingly dramatic change in the observed damage to the test specimens. The experimental points on the diagram indicate that the damage (i.e. permanent deflection) experienced by the model approximates to that predicted from the use of Roberts' approach.

SCALE UP

Baker (21) has described the scale-up of elastic, small and large plastic deflections of *structures subject to impulsive and shock loadings. The method, known as "geometric* scaling" allows a blast type loading to be scaled directly by a factor. If run number 135 is taken as an example. The following data is applicable.

Impulse (from reed anemometer)	=	0.62 kPa sec.
Height of replica	=	0.7 m
Distance from blast source	=	22.8 m
L/D ratio of column	=	36

By applying a geometric scaling factor of 10, the scaled values will be

Impulse	6.2 kPa sec.
Height	7m

Distance from blast epi-centre = 228 m

These values can now be compared with data taken from the Flixborough investigation. Taking a T.N.T. equivalent of 45t (15) then at 228 m from the source an impulse of 3.45 kPa sec. will act on a structure in the path of the blast.

From Roberts' work on 9 m high lamp-posts (L/D = 44) the pulses ranged up to 5.7 kPa sec. at distances between 50 and 260 m from the epi-centre and the angle of displacement ranged from 1 to 90 degrees.

RELEVANCE OF THE PULSE

The confine ment of the original gas/air mixture and the effects of interaction of the generated pressure pulse with the walls of the gallery might have meant that the pulse was dissimilar to a shock in air resulting from an industrial unconfined vapour cloud explosion. This possibility was examined using a hydraulic jump model i.e. relating a shock in air to a wave in water. Based on current models of unconfined vapour cloud explosions, the water model predicted that the pulse was similar to a shock in air (22).

CONCLUSIONS

Scale models of chemical plant were loaded by shock waves and deformed both elastically and plastically. The pressure versus time signatures of the generated pressure pulses compared favourably with those suggested by theories relating to unconfined vapour cloud explosions.

Roberts' approach was applied to permanently deformed models while a modified mode summation technique was used to analyse both elastic and plastic deformations. Within the inherent experimental scatter, the results were consistent with those calculated using the Roberts approach and with those from the mode summation technique for elastic deformations. It is evident that the drag loading phase of the pressure waves caused the observed deformations.

As expected, an increase in the L/D ratio of vertical columns leads to an increase in degree of deformation for a given loading. The addition of stiffening rings increased the resistance to blast but wind spoilers decreased the resistance.

The results agree with effects found after the incident at Flixborough. It is suggested however that present "models" for correlating blast damage associated with flammable gas/air mixtures may need improvement.

ACKNOWLEDGEMENTS

The authors wish to express their thanks to the Health and Safety Executive for financial support and practical assistance. In particular, they thank Dr. Alan Roberts, Dr. David Pritchard and Mr. John Turner for their continuous support and encouragement.

REFERENCES

(1) R. Strehlow; "Unconfined Vapour Cloud Explosions - an Overview". 14th Int. Symp. on combustion. Combustion Institute, Pittsburgh, Pennsylvania 1973.
(2) V.C. Marshall; "Port Hudson - Detonation or Deflagration?" The Chemical Engineer p573 August 1977
(3) J.H. Lee et al; "Blast Effects from Vapour Cloud Explosions" 11th Loss Prevention Symposium A.I.Ch.E. New York 1974
(4) British Standard No. 5500 "Unfired Fusion Welded Pressure Vessels" BSI 1976

Distance from blast epi-centre = 228 m

These values can now be compared with data taken from the Flixborough investigation. Taking a T.N.T. equivalent of 45t (15) then at 228 m from the source an impulse of 3.45 kPa sec. will act on a structure in the path of the blast.

From Roberts' work on 9 m high lamp-posts (L/D = 44) the pulses ranged up to 5.7 kPa sec. at distances between 50 and 260 m from the epi-centre and the angle of displacement ranged from 1 to 90 degrees.

RELEVANCE OF THE PULSE

The confine ment of the original gas/air mixture and the effects of interaction of the generated pressure pulse with the walls of the gallery might have meant that the pulse was dissimilar to a shock in air resulting from an industrial unconfined vapour cloud explosion. This possibility was examined using a hydraulic jump model i.e. relating a shock in air to a wave in water. Based on current models of unconfined vapour cloud explosions, the water model predicted that the pulse was similar to a shock in air (22).

CONCLUSIONS

Scale models of chemical plant were loaded by shock waves and deformed both elastically and plastically. The pressure versus time signatures of the generated pressure pulses compared favourably with those suggested by theories relating to unconfined vapour cloud explosions.

Roberts' approach was applied to permanently deformed models while a modified mode summation technique was used to analyse both elastic and plastic deformations. Within the inherent experimental scatter, the results were consistent with those calculated using the Roberts approach and with those from the mode summation technique for elastic deformations. It is evident that the drag loading phase of the pressure waves caused the observed deformations.

As expected, an increase in the L/D ratio of vertical columns leads to an increase in degree of deformation for a given loading. The addition of stiffening rings increased the resistance to blast but wind spoilers decreased the resistance.

The results agree with effects found after the incident at Flixborough. It is suggested however that present "models" for correlating blast damage associated with flammable gas/air mixtures may need improvement.

ACKNOWLEDGEMENTS

The authors wish to express their thanks to the Health and Safety Executive for financial support and practical assistance. In particular, they thank Dr. Alan Roberts, Dr. David Pritchard and Mr. John Turner for their continuous support and encouragement.

REFERENCES

(1) R. Strehlow; "Unconfined Vapour Cloud Explosions - an Overview". 14th Int. Symp. on combustion. Combustion Institute, Pittsburgh, Pennsylvania 1973.
(2) V.C. Marshall; "Port Hudson - Detonation or Deflagration?" The Chemical Engineer p573 August 1977
(3) J.H. Lee et al; "Blast Effects from Vapour Cloud Explosions" 11th Loss Prevention Symposium A.I.Ch.E. New York 1974
(4) British Standard No. 5500 "Unfired Fusion Welded Pressure Vessels" BSI 1976

FIGURE 1 P-I DIAGRAM FOR MODEL
(based on Roberts Approach)
L = 0.605m.

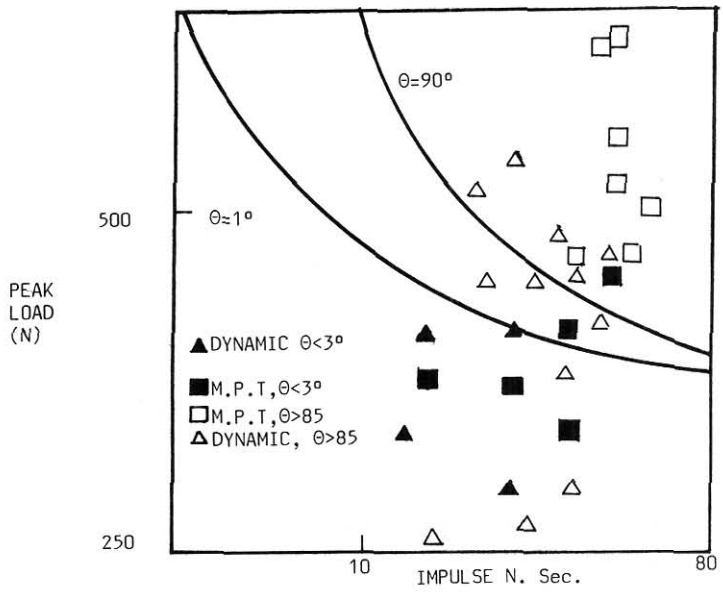

FIGURE 2 VARIATION OF L/D RATIO WITH LOADING
TO CAUSE SAME DEGREE OF DAMAGE

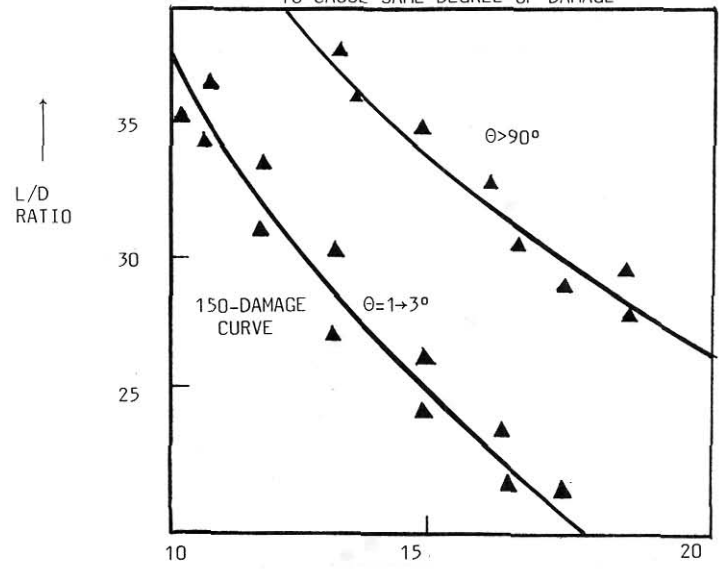

Figure 3 CALCULATED LOADINGS ACCORDING TO ROBERTS APPROACH VERSUS ACTUAL DYNAMIC LOADINGS FOR SMALL ANGLE DEFLECTIONS

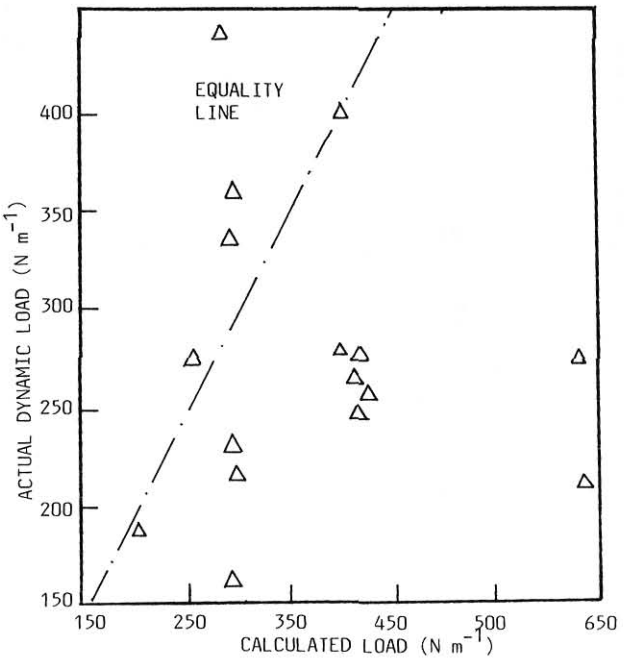

Figure 4 CALCULATED LOADINGS VERSUS LOADINGS TAKEN FROM MINIATURE PRESSURE TRANSDUCERS FOR SMALL ANGLE DEFLECTIONS

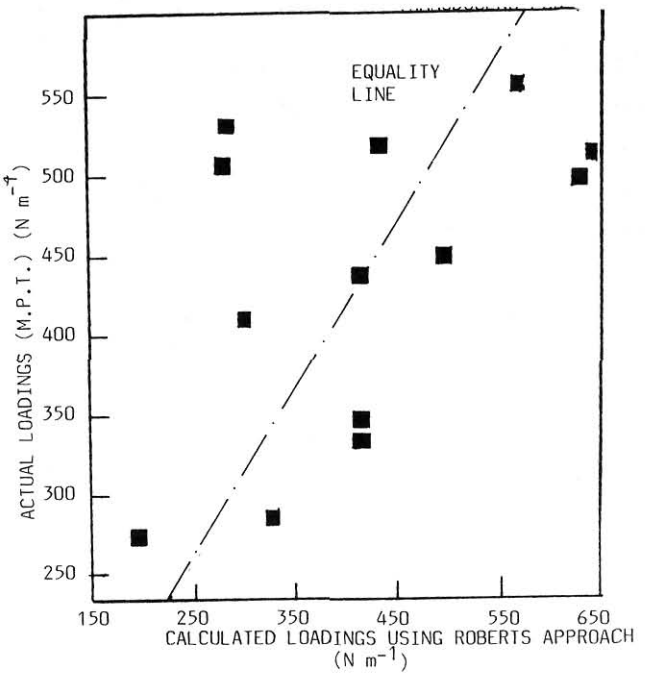

Figure 5 ELASTIC TIP DISPLACEMENTS FROM MODE SUMMATION METHOD VERSUS MEASURED ELASTIC TIP DISPLACEMENTS.

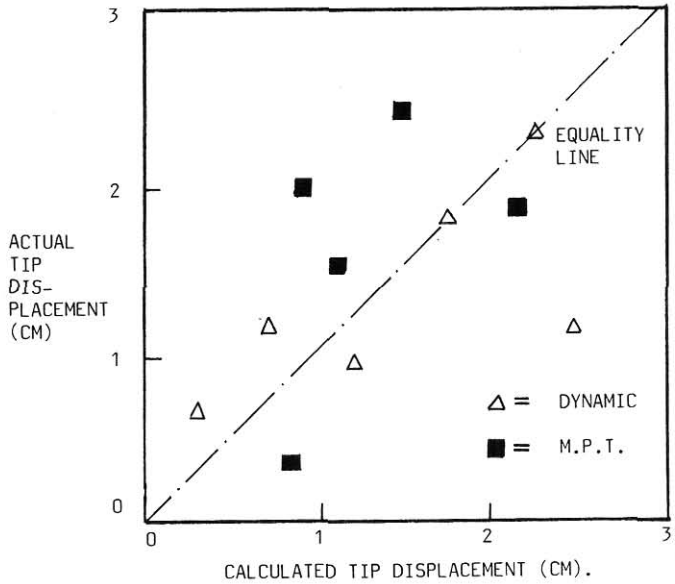

Figure 6 CALCULATED TIP DISPLACEMENT VERUS ACTUAL TIP DISPLACEMENT (SMALL ANGLE DEFLECTIONS).